HHS Public Access

Author manuscript

Science. Author manuscript; available in PMC 2015 March 02.

Published in final edited form as:

Science. 2014 August 15; 345(6198): 818–822. doi:10.1126/science.1255825.

Impaired Mucus Detachment Disrupts Mucociliary Transport in a Piglet Model of Cystic Fibrosis

Mark J. Hoegger[1], **Anthony J. Fischer**[2], **James D. McMenimen**[3], **Lynda S. Ostedgaard**[3], **Alex J. Tucker**[3], **Maged A. Awadalla**[3], **Thomas O. Moninger**[6], **Andrew S. Michalski**[3], **Eric A. Hoffman**[3,4,5], **Joseph Zabner**[3], **David A. Stoltz**[1,3,5,*], and **Michael J. Welsh**[1,3,7,*]

[1]Department of Molecular Physiology and Biophysics, University of Iowa, Roy J. and Lucille A. Carver College of Medicine, Iowa City, IA 52242

[2]Department of Pediatrics, University of Iowa, Roy J. and Lucille A. Carver College of Medicine, Iowa City, IA 52242

[3]Department of Internal Medicine, University of Iowa, Roy J. and Lucille A. Carver College of Medicine, Iowa City, IA 52242

[4]Department of Radiology, University of Iowa, Roy J. and Lucille A. Carver College of Medicine, Iowa City, IA 52242

[5]Department of Biomedical Engineering, University of Iowa, Roy J. and Lucille A. Carver College of Medicine, Iowa City, IA 52242

[6]Central Microscopy Research Facility, University of Iowa, Roy J. and Lucille A. Carver College of Medicine, Iowa City, IA 52242

[7]Howard Hughes Medical Institute, University of Iowa, Roy J. and Lucille A. Carver College of Medicine, Iowa City, IA 52242

Abstract

Lung disease in people with cystic fibrosis (CF) is initiated by defective host defense that predisposes airways to bacterial infection. People with advanced CF exhibit deficits in mucociliary transport (MCT), a process that traps and propels bacteria out of lungs, but whether this occurs first or is secondary to airway remodeling has been unclear. To assess MCT, we tracked movement of radiodense microdisks in airways of newborn CF piglets. Cholinergic stimulation, which elicits mucus secretion, caused microdisks to become stuck. Impaired MCT was not due to periciliary liquid depletion; rather, CF submucosal glands secreted mucus strands that remained tethered to gland ducts and hindered MCT. Inhibiting anion secretion in non-CF airways replicated CF abnormalities. These findings identify impaired MCT as a primary defect, link CFTR loss in submucosal glands to failure of mucus detachment from glands, and suggest that submucosal glands and tethered mucus may be targets for early CF treatment.

Mutations in the *CFTR* gene cause CF (1). Lung disease, the source of most mortality, arises from defective host defense that predisposes airways to bacterial infection. MCT defends

*Corresponding authors. david-stoltz@uiowa.edu; michael-welsh@uiowa.edu.

airways by trapping pathogens in mucus and cilia propel them out of the lung (2–4). Finding abnormal MCT in advanced CF (3) and some studies in culture (5) have led to the assumption that impaired MCT causes CF lung disease. Yet, *in vivo* data suggest that CF MCT defects may be secondary to inflammation and airway remodeling. For example, in some studies CF adults showed no MCT abnormality, and CF children exhibited no MCT defects (3, 6, 7). Moreover, as severity of CF lung disease increased, MCT deficits increased, and in other pulmonary diseases airway inflammation is also linked to MCT defects (8). Until now, lack of an animal model that replicates human CF and lack of sensitive MCT assays prevented ascertainment of whether MCT is impaired from the outset and thus contributes to pathogenesis or is a secondary defect.

A porcine CF model provides an opportunity to test MCT *in vivo* at the disease's origin (9). At birth, CF pig airways lack infection and inflammation, but spontaneously develop hallmark CF features including infection, inflammation, mucus accumulation and obstruction. To assay MCT *in vivo* with good spatial and temporal resolution, we developed an X-ray computed tomography-based assay to track movement of 350 μm diameter tantalum microdisks (10).

Most current MCT assays measure disappearance of radioactivity (clearance) after inhalation of radiolabeled particles (3, 6, 7). After insufflation into newborn piglet airways, a similar % of microdisks cleared CF and non-CF lungs in 10 min (Fig. 1A,1B,S1) (10). As microdisks were swept toward the larynx, they migrated to the ventral tracheal surface in both genotypes (Fig. 1C), consistent with our finding that ciliary orientation drives microdisks ventrally (10). Both genotypes propelled microdisks with similar maximal and mean speeds and microdisks spent a similar % of time moving (Fig. 1D–1F). Thus, under basal conditions, CF MCT appeared intact.

Airway insults can elicit a cholinergic reflex, a protective response that increases cilia beating and generates copious submucosal gland mucus secretion (4, 11, 12). The cholinergic agonist methacholine raised cilia beat frequency in CF and non-CF (Fig. S2A). However, it tended to reduce the % of microdisks that cleared CF lungs (Fig. 1A,1B, Video 1). Measuring individual microdisk behavior revealed that methacholine accelerated maximal and mean microdisk speeds in non-CF, but not CF piglets (Fig. 1D,1E, S1C–S1E). The most striking difference between genotypes was that in CF piglets, methacholine reduced the % of time individual microdisks were in motion by ~40% (Fig. 1F). Thus, rather than enhancing MCT and airway defense, a cholinergic agonist impeded MCT in CF piglets. A limitation of this *in vivo* study is that piglets were supine, anesthetized and did not cough; cholinergic stimulation might have produced a different response in awake animals.

Some studies of cultured airway epithelia reported that loss of CFTR increased Na^+ channel activity, causing excess liquid absorption from airway surfaces, decreased periciliary liquid, impaired cilia function, and thereby slowed MCT (5). However, culture models do not recapitulate the complexity of MCT because mucus cannot enter or escape cultures, and the model lacks submucosal glands, which are estimated to produce ~95% of mucus in large airways (4). After infusing methacholine, periciliary liquid depth did not differ by genotype (Fig. S2B), consistent with studies in CF pigs and humans (13, 14). However, mucus

overlying cilia was often dislodged during processing, and we could not assess potential effects of reduced volume secretion by CF submucosal glands (15, 16). Together, the results suggested that MCT might be disrupted by a CF abnormality in glands rather than surface epithelia. To test this, we flooded tracheas from methacholine-treated piglets with saline in a volume >1000-fold periciliary liquid volume (Fig. 2A, Video 2). This intervention prevents airway surface epithelia from altering the volume or composition of liquid covering airways.

Microdisks added to submerged non-CF airways rarely stopped as they progressed to the cranial and ventral edges (Fig. 2B, Video 2A,2B). In CF tracheas, some microdisks traveled like those on non-CF trachea. However, CF decreased the time that microdisks were in motion by ~50% (Fig. 2C), in good agreement with *in vivo* data (Fig. 1F). These results further excluded periciliary liquid depletion as the cause of impaired MCT. Moreover, on some occasions, we could see and remove CF mucus strands with attached microdisks (Video 2C).

To probe further for CF mucus abnormalities, we examined the response to methacholine because it elicited CF MCT defects *in vivo* and *ex vivo* (Fig. 1,2), and it stimulates submucosal gland secretion, consisting of liquid and proteins, including mucins, which confer key structural properties to mucus (11, 12). Cholinergic stimulation can also can activate CFTR, increase the driving force for anion secretion through CFTR, and thereby enhance liquid secretion (17, 18). To visualize mucus in real time, we covered excised tracheas with saline that contained a dilute suspension of fluorescent nanospheres (40 nm diameter) (Fig. 3A, Video 3).

When nanospheres attached to mucus, their increased local density highlighted strands and globules of mucus flowing over or linked to airways (Video 3A). Methacholine stimulated production of mucus strands that emanated from submucosal gland ducts and sometimes extended hundreds of μm from their anchor point (Fig. 3B, Video 3B). Strands grew in length from gland ducts (Fig. 3C). As mucus strands grew, they broke free and were carried up the airway (Fig. 3D, Video 3C). Mucus strands flowing over the surface sometimes attached to and stretched anchored strands. Then after the two strands separated, the attached strand often snapped back like a rubber band (Fig. 3E, Video 3D), indicating elasticity and tenacity, important mucus properties. Reflected light studies also revealed mucus strands emerging from submucosal gland ducts (Video 3E). Scanning electron microscopy and immunocytochemistry also identified mucus emerging from submucosal gland ducts (Fig. S3A,S3B).

Because our preliminary observations suggested more mucus attached to CF airways, we developed a time-averaging procedure to preferentially visualize stationary mucus and provide panoramic views of entire tracheal segments (Fig. 4A, S4, Video 4). During a 15 min basal period, stationary mucus was rarely detected on non-CF airways (Fig. 4B, Video 4A). After adding methacholine, nanosphere-labeled mucus was mobile and therefore not visualized; it only became apparent after accumulation on ventral and cranial edges of airway segments. Under basal conditions, the surface of CF trachea revealed only small amounts of stationary mucus. However, methacholine stimulation generated a strikingly different appearance, with many immobile mucus strands and globules failing to detach

from submucosal gland ducts (or attaching to anchored strands) and not flowing across the airway (Fig. 4C,4E,S5, Video 4B).

Failure of mucus to detach, despite being bathed in saline of controlled composition, indicated that CF mucus was abnormal before it emerged onto the airway surface. That result pointed to a defect in submucosal glands; they express abundant CFTR (19, 20) and conduct Cl^- and HCO_3^- (21) that contribute to liquid secretion (11, 17, 22, 23). To test if loss of anion transport might be responsible for altered mucus behavior in CF, we bathed non-CF trachea in HCO_3^--free saline or saline containing bumetanide, which inhibits basolateral Cl^- entry into epithelia (23). Neither alone caused a failure of mucus detachment (Fig. S6). However when combined, they reproduced the CF phenotype of tethered mucus strands and globules (Fig. 4D,4F, Video 4C). Tracing mucus strands to their source revealed submucosal gland ducts as their origin (Video 4D). Because ion transport by epithelia lining airways would not alter the composition of liquid covering the surface, these changes can be attributed to reduced anion secretion into submucosal gland lumens. The results are also consistent with previous findings that inhibiting both Cl^- and HCO_3^- secretion altered viscoelastic properties of submucosal gland secretions (4, 24).

To explore whether mucus impeded movement of the microdisks we used *in vivo* (Fig. 1), we applied them to non-CF epithelia in HCO_3^--free saline plus bumetanide and found that they failed to move across the surface. Then, adding fluorescent nanospheres revealed microdisks attached to mucus (Fig. 4G, Video 4E). Similar results occurred in CF airways (Fig. 4H, Video 4F).

Our findings identify impaired mucus detachment from CF submucosal glands as a primary defect that disrupts MCT. Na^+ hyperabsorption by airway surface epithelia and periciliary liquid depletion (5) do not explain the data. These *in vivo* and *ex vivo* results link loss of CFTR and reduced anion secretion to altered mucus that has a reduced ability to break free after emerging from glands. Reduced Cl^- and HCO_3^--dependent liquid secretion (23, 24) and reduced HCO_3^- secretion (or acidic pH) (25–27) have both been proposed to alter CF mucus properties. Our data suggest that neither alone may be sufficient to generate abnormal CF mucus.

These plus our earlier results (28) reveal that loss of CFTR disrupts two lung defense processes, MCT and secreted antimicrobial activity. Vertebrates and invertebrates employ these two defenses at point of contact with environmental pathogens. CF does not eliminate either defense, but reduces their effectiveness. A vicious cycle caused by partial disruption of two processes may, in part, explain greater severity of lung disease in CF compared to primary ciliary dyskinesia, which obliterates MCT (29), because compromising one defense may accentuate the other defect. For example, mucus that fails to detach would impair MCT and provide a nidus for bacteria to grow under conditions that promote resistance to host defenses already weakened by CF (28, 30). Conversely, reduced antibacterial activity could precipitate infection that triggers submucosal gland secretion, and defective mucus detachment would impair MCT. Inflammation resulting from both defects would evoke submucosal gland hypertrophy, further increasing the amount of static mucus. Now that newborn CF screening is universal in many countries, there is an opportunity to intervene

early. These data suggest that submucosal glands and mucus tethered to them may be targets for early treatment and that MCT assays could report therapeutic efficacy.

Supplementary Material

Refer to Web version on PubMed Central for supplementary material.

Acknowledgments

We thank Mahmoud Abou Alaiwa, Ryan J. Adam, Elizabeth Allard, Lucas A. Askland, Drake C. Bouzek, Kathryn Chaloner, Nick D. Gansemer, Omar A. Itani, Theresa A. Mayhew, Sean Mobberley, John H. Morgan, Leah R. Reznikov, Jered Sieren, Mallory R. Stroik, Peter J. Taft, and Tanner J. Wallen for valuable assistance and discussions. This work was supported by the NIH (HL051670, HL091842, DK054759), the Carver Foundation, and the Cystic Fibrosis Foundation. DAS is supported by the Gilead Sciences Research Scholars Program in Cystic Fibrosis and the NIH (DP2 HL117744). AJF is supported by a CFF Fellowship. MJW is an Investigator of the HHMI.

References and Notes

1. Welsh, MJ.; Ramsey, BW.; Accurso, F.; Cutting, GR. The Metabolic and Molecular Basis of Inherited Disease. Scriver, CR.; Beaudet, AL.; Sly, WS.; Valle, D.; Childs, B.; Vogelstein, B., editors. McGraw-Hill; New York: 2001. p. 5121-5189.
2. Wanner A, Salathe M, O'Riordan TG. 1996; 154:1868–1902.
3. Robinson M, Bye PT. Pediatr Pulmonol. 2002; 33:293–306. [PubMed: 11921459]
4. Wine JJ, Joo NS. Proc Am Thorac Soc. 2004; 1:47–53. [PubMed: 16113412]
5. Boucher RC. J Intern Med. 2007; 261:5–16. [PubMed: 17222164]
6. McShane D, Davies JC, Wodehouse T, Bush A, Geddes D, Alton EW. Eur Respir J. 2004; 24:95–100. [PubMed: 15293610]
7. Regnis JA, Robinson M, Bailey DL, Cook P, Hooper P, et al. Am J Respir Crit Care Med. 1994; 150:66–71. [PubMed: 8025774]
8. Fahy JV, Dickey BF. N Engl J Med. 2010; 363:2233–2247. [PubMed: 21121836]
9. Stoltz DA, Meyerholz DK, Pezzulo AA, Ramachandran S, Rogan MP, et al. Sci Transl Med. 2010; 2:29ra31.
10. Hoegger MJ, Awadalla M, Namati E, Itani OA, Fischer AJ, et al. Proc Natl Acad Sci U S A. 2014; 111:2355–1260. [PubMed: 24474805]
11. Ballard STD. Respir Physiol Neurobiol. 2007; 159:271–277. [PubMed: 17707699]
12. Wine JJ. Auton Neurosci. 2007; 133:35–54. [PubMed: 17350348]
13. Chen JH, Stoltz DA, Karp PH, Ernst SE, Pezzulo AA, et al. Cell. 2010; 143:911–923. [PubMed: 21145458]
14. Griesenbach U, Soussi S, Larsen MB, Casamayor I, Dewar A, et al. Am J Respir Cell Mol Biol. 2010; 44:309–315. [PubMed: 20418361]
15. Joo NS, Cho HJ, Khansaheb M, Wine JJ. J Clin Invest. 2010; 120:3161–3166. [PubMed: 20739758]
16. Wu DXY, Lee CYC, Uyekubo SN, Choi HK, Bastacky SJ, JH. Am J Physiol. 1998; 274:L388–L395. [PubMed: 9530174]
17. Billet A, Hanrahan JW. J Physiol. 2013; 591:5273–5278. [PubMed: 23959675]
18. Lee RJ, Foskett JK. J Biol Chem. 2012; 287:38316–38326. [PubMed: 22989883]
19. Engelhardt JF, Yankaskas JR, Ernst SA, Yang Y, Marino CR, et al. Nat Genet. 1992; 2:240–248. [PubMed: 1285365]
20. Lee RJ, Harlow JM, Limberis MP, Wilson JM, Foskett JK. J Gen Physiol. 2008; 132:161–183. [PubMed: 18591422]
21. Poulsen JH, Fischer H, Illek B, Machen TE. Proc Natl Acad Sci U S A. 1994; 91:5340–5344. [PubMed: 7515498]

22. Moon S, Singh M, Krouse ME, Wine JJ. Am J Physiol. 1997; 273:L1208–L1219. [PubMed: 9435576]
23. Trout L, Gatzy JT, Ballard ST. Am J Physiol. 1998; 275:L1095–1099. [PubMed: 9843846]
24. Ballard ST, Inglis SK. J Physiol. 2004; 556:1–10. [PubMed: 14660706]
25. Quinton PM. Lancet. 2008; 372:415–417. [PubMed: 18675692]
26. Quinton PM. Am J Physiol. 2010; 299:C1222–1233.
27. Gustafsson JK, Ermund A, Ambort D, Johansson ME, Nilsson HE, et al. J Exp Med. 2012; 209:1263–1272. [PubMed: 22711878]
28. Pezzulo AA, Tang XX, Hoegger MJ, Alaiwa MH, Ramachandran S, et al. Nature. 2012; 487:109–113. [PubMed: 22763554]
29. Cohen-Cymberknoh M, Simanovsky N, Hiller N, Gileles Hillel A, Shoseyov D, Kerem E. Chest. 2014; 145:738–744. [PubMed: 24091606]
30. Staudinger BJ, Muller JF, Halldorsson S, Boles B, Angermeyer A, et al. Am J Respir Crit Care Med. 2014; 189:812–824. [PubMed: 24467627]
31. Rogers CS, Stoltz DA, Meyerholz DK, Ostedgaard LS, Rokhlina T, et al. Science. 2008; 321:1837–1841. [PubMed: 18818360]
32. Amirav I, Kramer SS, Grunstein MM, Hoffman EA. J Appl Physiol. 1993; 75:2239–2250. [PubMed: 8307884]
33. Sims DE, Horne MM. Am J Physiol. 1997; 273:L1036–L1041. [PubMed: 9374732]
34. Matsui H, Grubb BR, Tarran R, Randell SH, Gatzy JT, et al. Cell. 1998; 95:1005–1015. [PubMed: 9875854]
35. Bartlett JA, Albertolle ME, Wohlford-Lenane C, Pezzulo AA, Zabner J, et al. Am J Physiol. 2013; 305:L256–626.
36. Meyerholz DK, Stoltz DA, Namati E, Ramachandran S, Pezzulo AA, et al. Am J Respir Crit Care Med. 2010; 182:1251–1261. [PubMed: 20622026]

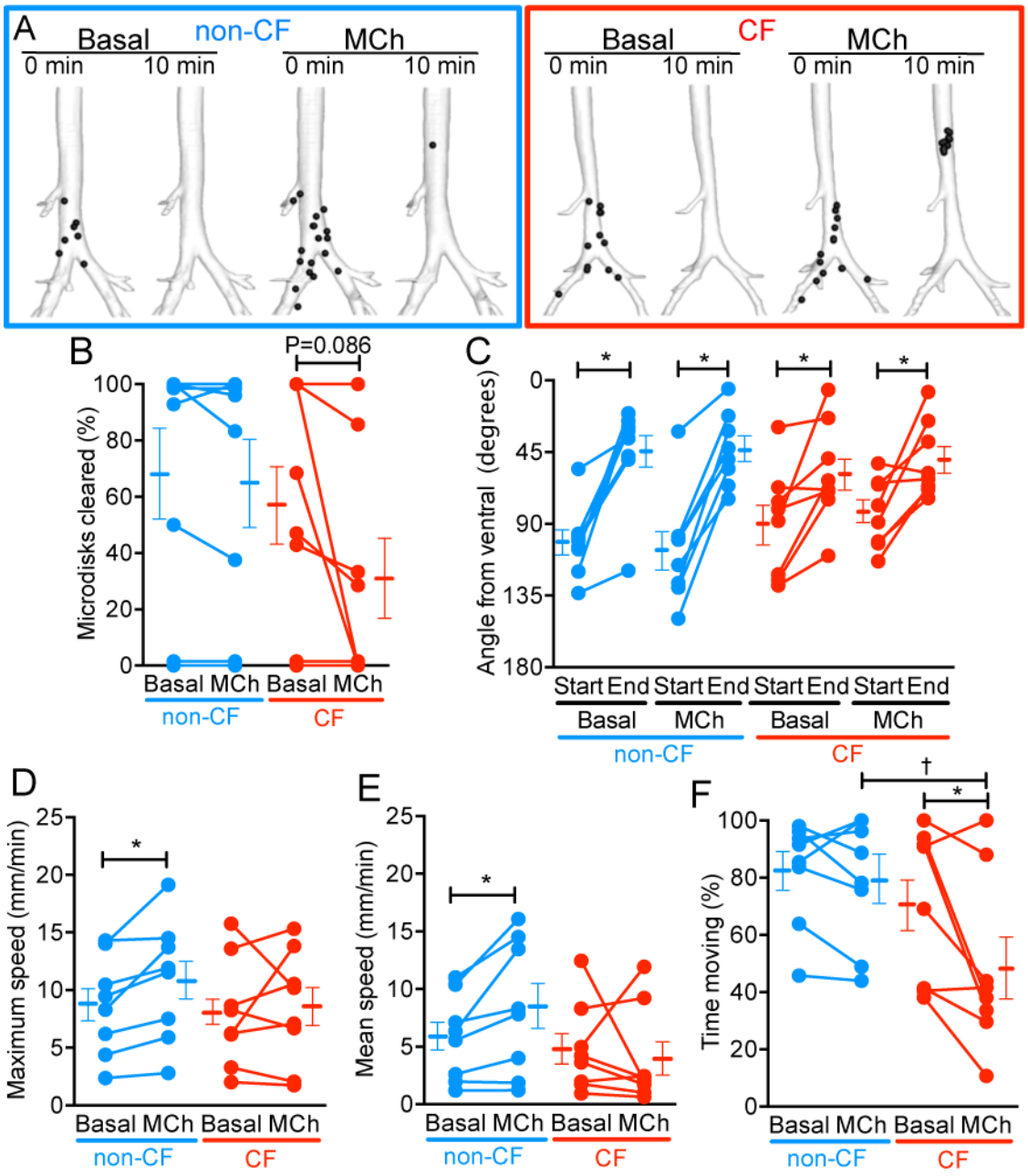

Fig. 1. Loss of CFTR impairs MCT *in vivo* in newborn piglets treated with methacholine

(**A**) Images are reconstructed ventral-dorsal views of non-CF and CF airways under basal conditions and after 1.28 $\times 10^{-7}$ mol/kg, IV methacholine. Images are at beginning and end of a 10 min tracking period (Videos 1A,1B). Positions of microdisks are shown as spheres (enlarged ~40 times actual area). (**B to F**). Symbols indicate data from 8 non-CF and 8 CF piglets studied before and after 1.28 $\times 10^{-7}$ mol/kg, IV methacholine. Each data point is average behavior of individual microdisks in a piglet during a 10 min tracking run. Lines and whiskers beside individual data are mean±SEM. * indicates P<0.05, paired Student's *t*-test. (**B**) Percentage of microdisks that cleared tracking field during 10 min tracking period. (**C**) Radial position of microdisks at start and end of 10 min tracking period. Data are

absolute values of angles relative to ventral (0 degrees). (**D,E**) Maximum and mean speed of microdisks. (**F**) Percentage of time microdisks were moving during a tracking run. † indicates P<0.05 unpaired Student's *t*-test. Analysis using linear mixed effects model with random effect for pigs yielded a similar conclusion (P=0.024). Analysis in panel F was not adjusted for multiple comparisons.

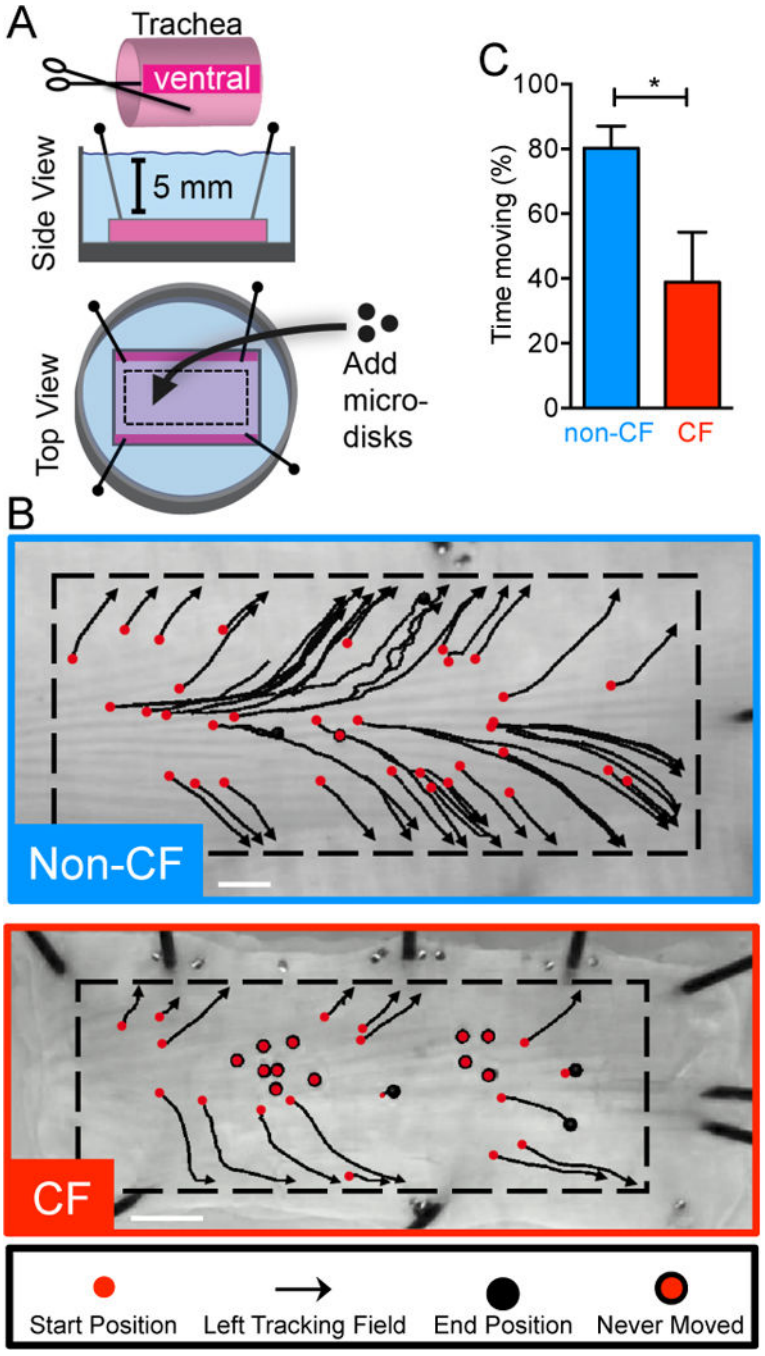

Fig. 2. Loss of CFTR increases the percentage of non-mobile microdisks on *ex vivo* trachea submerged in saline

(**A**) Schematic showing trachea removed from piglets treated with methacholine (1.28×10^{-5} mol/kg, IV), opening along the ventral surface, covering with saline, application of tantalum microdisks to the surface, and tracking of movement. Images in panel B are examples and data in panel C are averages. (**B**) Track of microdisks. Red circle indicates microdisk start position. Arrowhead indicates position of tracking field exit. Black circle indicates end position of microdisk that failed to clear tracking field. Red/black circle indicates disk that

never moved. Dashed line indicates tracking field. Bar = 2 mm. Images are compiled from a 10 min tracking period (Videos 2A,2B). (**C**) Percentage of time microdisks were moving. N = 4 non-CF and 4 CF tracheas. * P<0.05 unpaired Student's *t*-test.

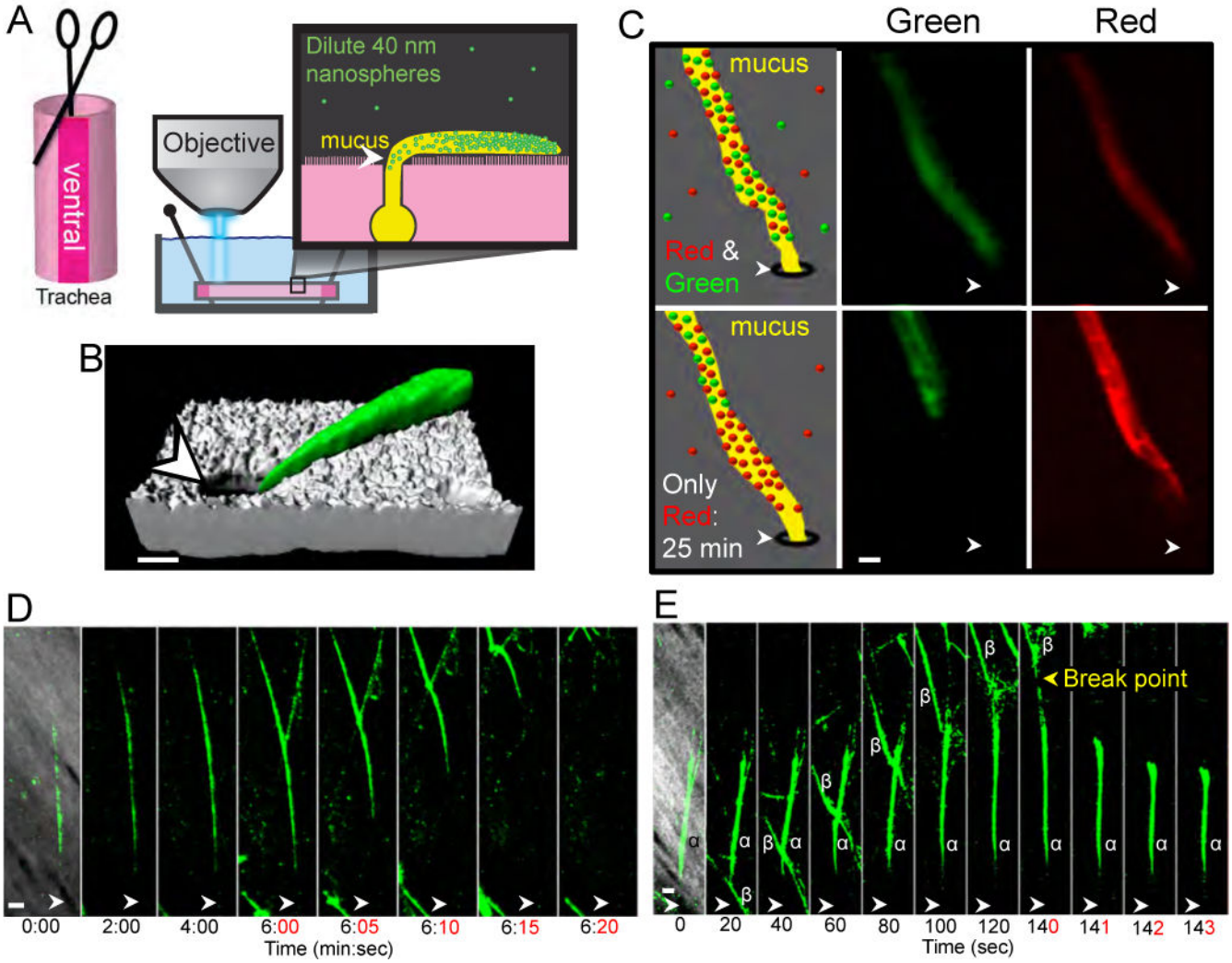

Fig. 3. Strands of mucus emerge from submucosal gland ducts in methacholine-treated non-CF airways studied *ex vivo*

Submucosal gland duct openings are indicated by arrowheads. (**A**) Schematic of imaging procedure. All experiments were repeated at least 3 times. Non-CF trachea was removed from piglets, opened along ventral surface, pinned flat, submerged in a HCO_3^-/CO_2 buffered Ringers, and treated with 1.28×10^{-5} mol/L methacholine. Trachea was opened along ventral surface so that cilia would propel mucus and nanospheres to lateral edges of the tracheal preparation (10). Solution bathing the trachea contained a dilute suspension of fluorescent 40 nm nanospheres. Images were obtained with a high-speed confocal microscope at the tracheal surface. Green indicates fluorescence from nanospheres (Video 3A). (**B**) Reconstruction of mucus (labeled with green nanospheres) emerging from submucosal gland duct onto airway surface (grey) (Video 3B). Bar = 50 μm. (**C**) Mucus strands grow in length from submucosal glands. In top panels, saline contained dilute suspension of green and red nanospheres, and both labeled a mucus strand. Green nanospheres were then removed from saline and mucus strand continued to elongate from gland duct as indicated by labeling with red nanospheres in bottom panels 25 min later. Bar

= 50 μm. (**D**) Mucus strand grew from opening of submucosal gland duct and then broke free and rapidly flowed out of microscopic field (Video 3C). Time is at bottom. Grey background in first panel is reflected light image. Bar = 50 μm. (**E**) Mucus strand "α", anchored at arrowhead, temporarily captures another mucus strand "β" flowing past, α stretches, and then the connection between α and β breaks at 140 sec. Immediately after the break, β leaves the field, and α snaps back to its original length (Video 3D). Grey background in first panel is reflected light image. Bar = 50 μm.

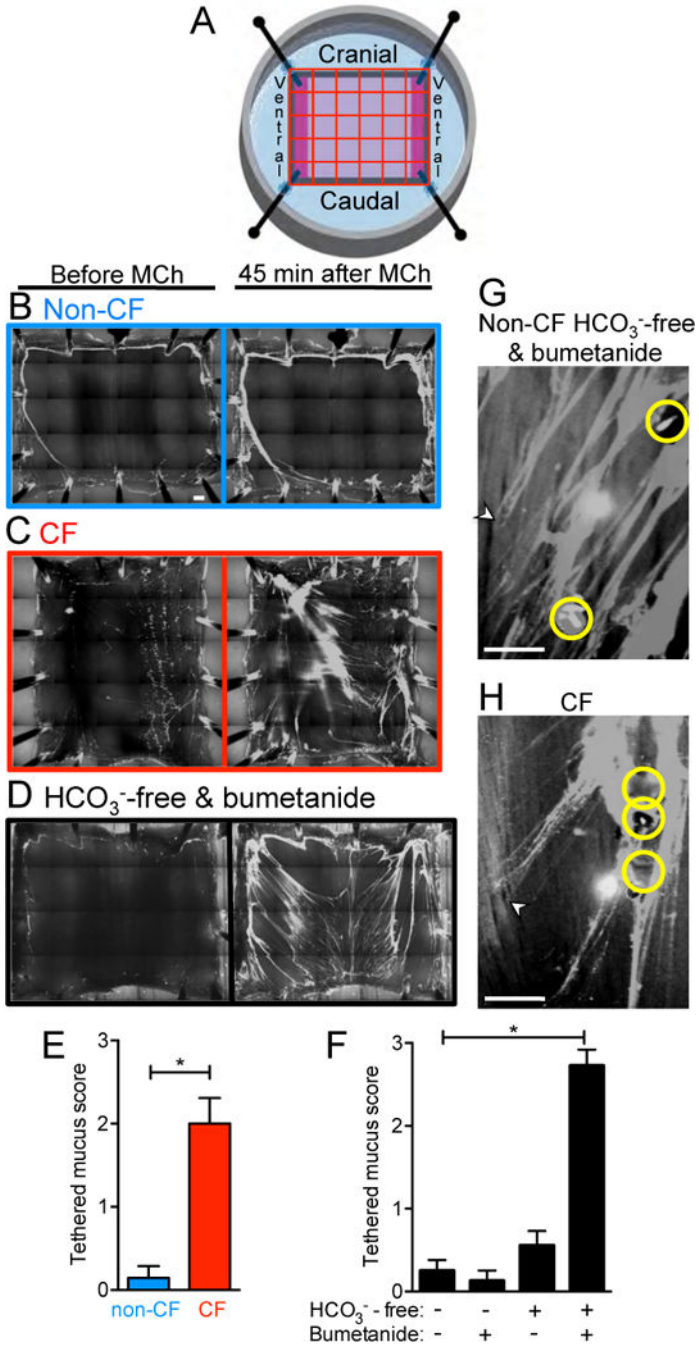

Fig. 4. Mucus strands fail to detach from submucosal glands when *ex vivo* CF airways are treated with methacholine or when liquid secretion is inhibited in non-CF airways

(**A**) Schematic of imaging procedure. Images are panoramic views of tracheal sections obtained with a time-averaging technique that visualizes static mucus labeled with fluorescent nanospheres. See Fig. S4, Video 4. Black lines on sides of images are pins holding trachea. Fluorescently-labeled mucus is shown in grey-scale. Panels B to D represent images from individual tracheas and average data and numbers of experiments are in panels E and F. (**B to D**) Airways were removed from methacholine-treated (1.28×10^{-5}

mol/kg, IV) piglets and images were captured at end of a 15 min basal period and then 45 min after adding 1.28×10^{-5} mol/L methacholine. Bar = 1 mm. See videos 4A to 4C. (**B**) Non-CF trachea. Note accumulation of mucus (white) along cranial and ventral edges of tissue. Some static mucus on lower left of non-CF trachea was attached to pin at tissue edge. (**C**) CF trachea. (**D**). Non-CF airways stimulated with methacholine in HCO_3^--free HEPES-buffered (pH 7.4 or 6.8) saline containing 10 μM bumetanide. (**E**) Mucus tethered to submucosal glands on non-CF and CF airways 45 min after adding methacholine. See Methods for description of tethered mucus score. N=7 non-CF and 7 CF trachea, * $P<0.05$ unpaired Student's *t*-test. (**F**) Mucus tethered to submucosal glands on non-CF trachea 45 min after adding methacholine. Trachea were bathed in HCO_3^-/CO_2-buffered saline (N=12), HCO_3^-/CO_2-buffered saline containing 10 μM bumetanide (N=8), HCO_3^--free HEPES-buffered (pH 7.4 or 6.8) saline (N=9), or HCO_3^--free saline containing bumetanide (N=11). * $P<0.05$ by one-way ANOVA and Bonferroni post-test. (**G,H**) Combined reflected light and fluorescence images show position of tantalum microdisks (yellow circles) and mucus; mucus often wrapped around microdisks and partly obscured them. Microdisks were applied to non-CF trachea in HCO_3^--free saline containing bumetanide (**G**) and to CF trachea (**H**). Subsequent addition of fluorescent nanospheres to saline revealed that all stationary microdisks were attached to mucus. These data also indicate that mucus strands formed independently of nanospheres. Arrowheads indicate submucosal gland ducts. Experiments were repeated at least 3 times. Bar = 1 mm. Video 4E,4F.